Article

Radiation Beam width and Beam direction electronical control of Transparent and Compact Vivaldi Antennas

Amani CHERIF[1,2], Mohamed HIMDI[1], Xavier CASTEL[1], Quentin SIMON[1], Saber DAKHLI[2], Fethi CHOUBANI[2]

[1] University Rennes, CNRS, IETR, UMR 6164, F-35000 Rennes, France, mohamed.himdi@univ-rennes.fr
[2] University of Tunis El Manar, Sup'Com, Tunis, Tunisia

Abstract: A printed Vivaldi antenna that is optically transparent, ultra-wideband (UWB), and reconfigurable has been developed, fabricated, and tested at millimeter wave frequencies. It covers a broad frequency range of 20-30 GHz by using three PIN diodes. The diodes control the current flow to direct the beam of the antenna. The results of numerical simulations and measurements match at millimeter wave frequencies. The design of this antenna is unique as it allows for a reduction in size and ease of integration while also providing the ability to change the radiation pattern by up to 300 degrees, making it suitable for 5G and 6G communications. Additionally, this antenna can also be useful for RF applications that require dynamic switching of radiation patterns and cognitive radio.

Keywords: Optical transparency, Vivaldi antenna, Active antenna, Reconfigurability, Wide band frequency.

1. INTRODUCTION

Designing and creating reconfigurable antennas that have a broad operating frequency range, are small in size, and have a soft visual impact are a very exciting challenge. One of the key advantages of optically transparent and reconfigurable printed Vivaldi antennas is that they can be integrated into a wide range of applications, such as smart windows, and smart glasses, without affecting the appearance of the device. Additionally, because they can be reconfigured to operate at different frequencies, they can be used for multiple wireless communication standards, such as 5G and 6G. Additionally, because the antenna can be reconfigured, it can be tuned to operate at different frequencies, making it more versatile than traditional fixed-frequency antennas. [1-4]. The trend in recent years has been to develop broadband frequency antennas or reconfigurable antennas that can serve multiple microwave applications from a single device. These antennas can be used for GPS, GSM, WLAN, and Bluetooth applications [5-8]. Additionally, 5G base stations require compact, reconfigurable antennas that can adjust radiation patterns to track users. This paper will describe the proposed transparent, reconfigurable, and broadband Vivaldi antenna in Section II, detail the fabrication process and characterization at microwaves in Section III, discuss experimental results in Section IV, and conclude in Section V.

2. Antenna design

The proposed reconfigurable wideband Vivaldi antenna was printed on a 25.4 mm x 25.4 mm x 0.2 mm fused quartz substrate (dielectric permittivity $\varepsilon_r = 3.75$ and loss tangent $\tan\delta = 4\text{x}10^{-4}$ at 24 GHz). It consisted of a 7.25 mm x 8.94 mm radiating element made of 2 distinctive parts (namely petals) and a specially designed ground plane that was printed on the front side of the substrate (Fig. 1a). The radiating element is energized by a transition between a slot and a micro strip line, which has a width of 3.1 mm and ends with a

Preprints (www.preprints.org) | NOT PEER-REVIEWED | Posted: 10 May 2023 doi:10.20944/preprints202305.0765.v1

quarter circle with a radius of 0.6 mm, which is printed on the back side of the fused quartz substrate (as shown in Figure 1b). On the front side of the substrate, three PIN diodes were integrated into tapered slot lines to achieve reconfigurable radiation patterns (as shown in Figure 1a). The slot line along the y-axis is terminated with a circular slot with a radius of 0.22 mm (as shown in Figure 1b).

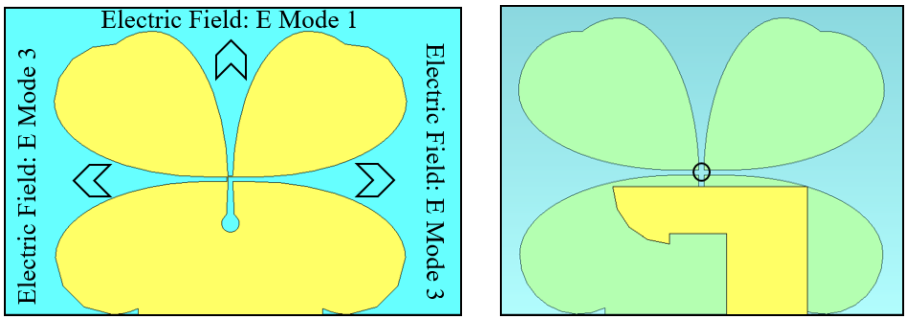

(a) (b)

Fig. 1. Detailed view of the front side of the printed Vivaldi antenna, including a close-up of the three PIN diodes **(a)** and an illustration of the micro strip feeding line on the back side **(b)**.

Table 1. Configuration modes

Modes	Diodes state		
	D1	D2	D3
Mode 1	ON	ON	OFF
Mode 2	OFF	ON	ON
Mode 3	ON	ON	OFF

Three PIN diodes, labeled D1, D2, and D3, are used to control the reconfigured slots to operate in three different modes. Mode 1 is achieved when D1 and D2 are in the ON state (acting as a short-circuit) and D3 is in the OFF state (acting as an open-circuit). Mode 2 is achieved when D2 and D3 are in the ON state and D1 is in the OFF state, and Mode 3 is achieved when D1 and D3 are in the ON state and D2 is in the OFF state. This is summarized in Table I.

The current flow through the tapered slots is maximized at the edges (as seen in Figs. 2a, 2c, and 2e) and the direction of the radiating beam can be adjusted by directing the current through D1, D2, or D3 PIN diodes. In Mode 1, with D1 and D2 in the ON state, the beam radiates at an angle of $\phi = 90°$ (as shown in Fig. 2b). In Mode 2, the deviation of the current occurs on the left side of the tapered slot (as shown in Fig. 2c) and in Mode 3, the deviation occurs on the right side (Fig. 2e).

The radiation pattern of the Vivaldi antenna can be adjusted to cover a 300° by utilizing the three different modes, allowing for greater control and flexibility.

Mode 1, shown in Fig. 2b, has the highest gain of 5.9 dBi at 26 GHz, while Modes 2 and 3, shown in Fig. 2d and 2f respectively, have lower gains of 3.2 dBi and 3.6 dBi in the same frequency. The difference in gain values is a result of greater back-side radiation in Modes 2 and 3. It should be noted that the simulations were conducted using a continuous silver metal layer. Figs 3 and 4 present the simulation outcomes of gain and efficiency for the three modes, which indicate a gain variation from 3.2 dBi to 5.9 dBi and efficiency from 80% to 92% at 26 GHz frequency.

Preprints (www.preprints.org) | NOT PEER-REVIEWED | Posted: 10 May 2023 doi:10.20944/preprints202305.0765.v1

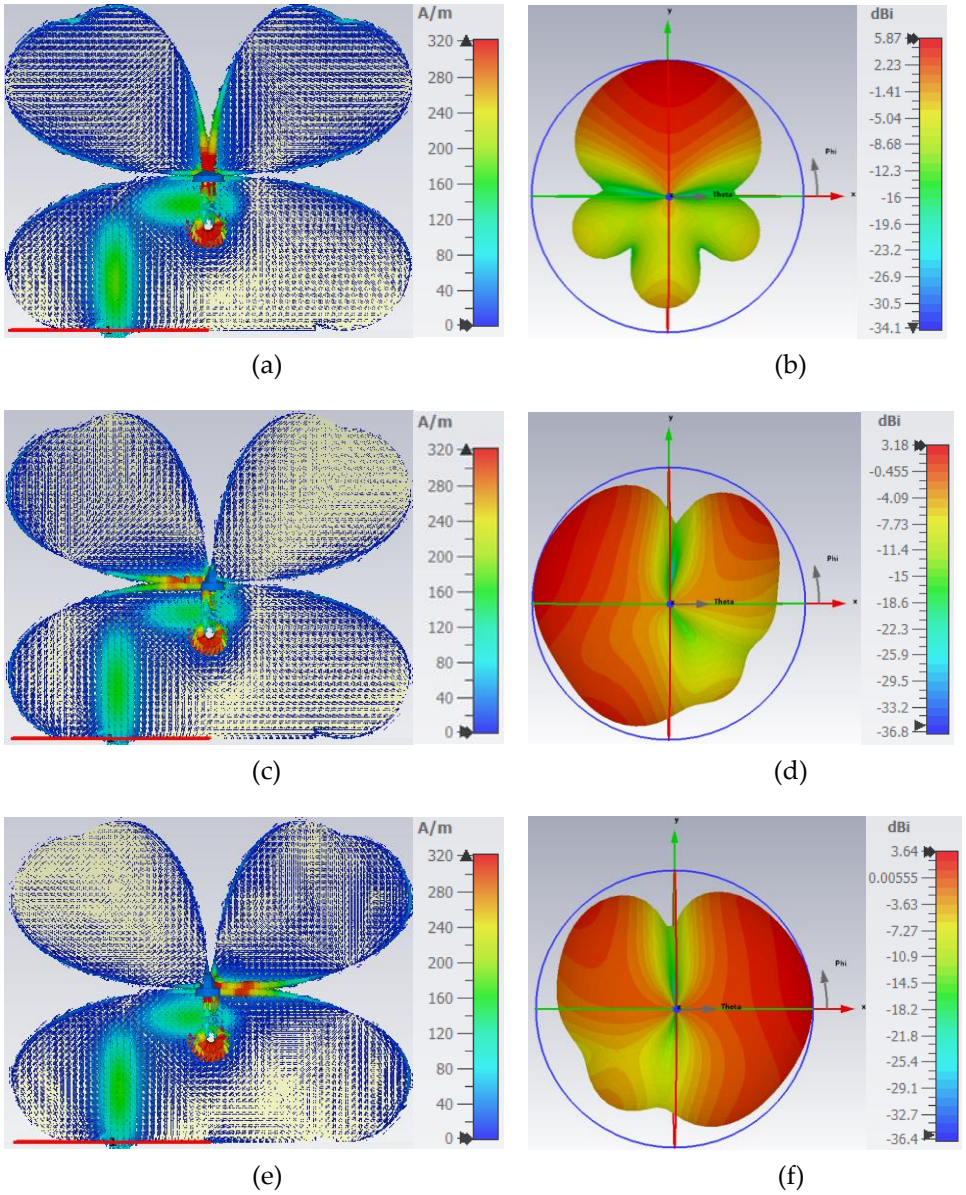

Fig. 2. Printed Vivaldi antenna with the surface current distribution in the Mode 1 **(a)**; Mode 2 **(c)**; Mode 3 **(e)** and the 3D radiation pattern at 26 GHz in the Mode 1 with θ_{-3dB}=72.3° **(b)**; Mode 2 with θ_{-3dB} -3dB=147° **(d)** and Mode 3 with θ_{-3dB} -3dB=127° **(f)**.

3. Simulations Results

Due to the PIN diode used MA4AGP907 (beam-lead), all simulations consider the perfect PIN diode behavior (ON=Open circuit, OFF=Short-circuit). The S parameters are shown in figure 3, and correspond to very good matching antenna for the three modes.

Preprints (www.preprints.org) | NOT PEER-REVIEWED | Posted: 10 May 2023 doi:10.20944/preprints202305.0765.v1

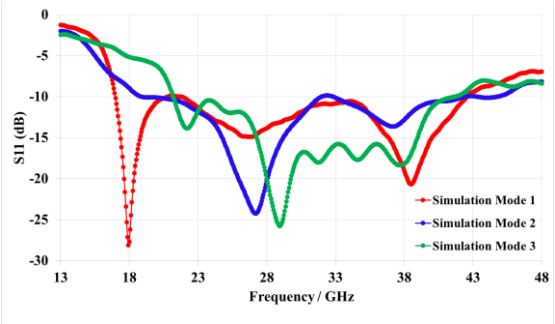

Fig. 3. Reflection coefficient magnitude of the transparent antenna operating in Mode 1, 2 and 3

Figure 4 illustrates the simulation results of the gain and efficiency performance in the three different modes, Mode 1, Mode 2, and Mode 3 of the antenna across a frequency range of 21-30 GHz.

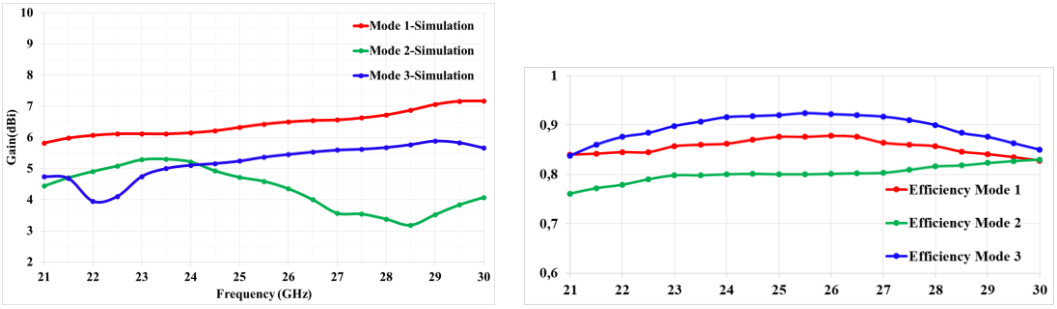

(a) (b)

Fig.4. Simulated gains **(a)** and efficiency **(b)** of the three modes of the printed Vivaldi antenna

4. Transparent Vivaldi Antenna Fabrication

Three transparent mesh antennas have been created using a process described in [4], which involves depositing a 1.35 μm-thick continuous silver film and a 5 nm-thick titanium adhesion film on a substrate using RF sputtering. Photolithographic wet etching is then used to create the antenna patterns with appropriate photomasks. The silver film was made three times thicker than the skin depth value (0.45 μm at 26 GHz) by using standard photolithographic wet etching processes and appropriate photomasks. During the photolithography process, careful alignment of the photomasks and the substrate is crucial to ensure the accuracy of the antenna. The resulting antenna is optically transparent, making it suitable for use in applications where visibility is important, such as in smart windows or heads-up displays. The distance between the antenna elements (pitch) affects the level of optical transparency, with wider pitch resulting in higher transparency levels (ranging from 66% to 89%). This transparency is measured using a UV-Visible spectrophotometer. The process of creating a transparent antenna involves creating square apertures in the metal layers, with a specific pitch and metal strip width. In this case, the pitch is 150 μm and the metal strip width is close to 15 μm. Fig. 5 details such an antenna.

Preprints (www.preprints.org) | NOT PEER-REVIEWED | Posted: 10 May 2023 doi:10.20944/preprints202305.0765.v1

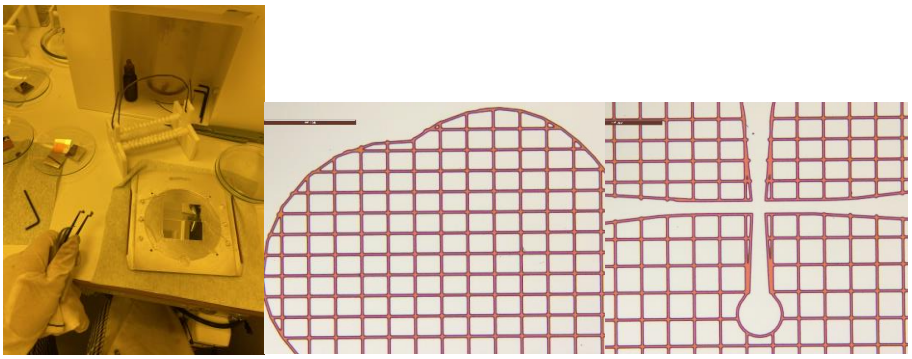

(a) (b)

Fig. 5. Fabricated transparent antenna: zoomed view by optical microscopy (scale bar = 500 μm) of a mesh petal **(a)** and ground with the petals **(b).**

5. Active transparent antenna

Three positive-intrinsic-negative (PIN) MA4AGP907 diodes were implemented as switches to provide the antenna beam switching (Fig. 6, and 7). PIN diodes are implemented as switches to provide beam switching capabilities and are connected in series to use only two DC supply voltages (V1 and V2) for the different modes is displayed in Table II. 200 μm-width biasing lines are positioned perpendicularly to minimize their impact on the radiation pattern, for each DC biasing line an inductors (L = 6 nH) and resistors (R = 100 Ω) are also used to block RF current and protect the diodes, respectively.

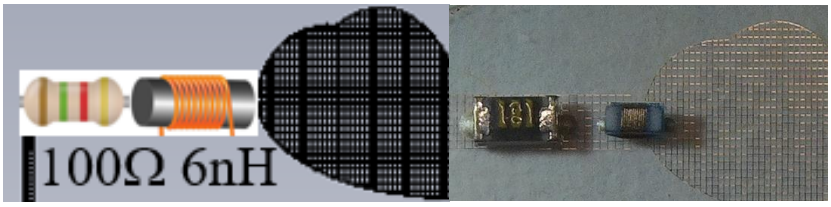

(a) (b)

Fig. 6. Diagram of the inductor and resistor positions **(a)** detail of the fabricated Vivaldi antenna with the inductor and resistor **(b)**

As indicated in table 2, to activate Mode 1, apply reverse bias to D1 and forward bias to D2 and D3. For Mode 2, apply reverse bias to D2 and forward bias to D1 and D3. And, for Mode 3, apply reverse bias to D3 and forward bias to D1 and D2. Modes 1, 2, and 3 refer to activation of upper radiating slot, left-sided slot, and right-sided slot respectively.

Preprints (www.preprints.org) | NOT PEER-REVIEWED | Posted: 10 May 2023 doi:10.20944/preprints202305.0765.v1

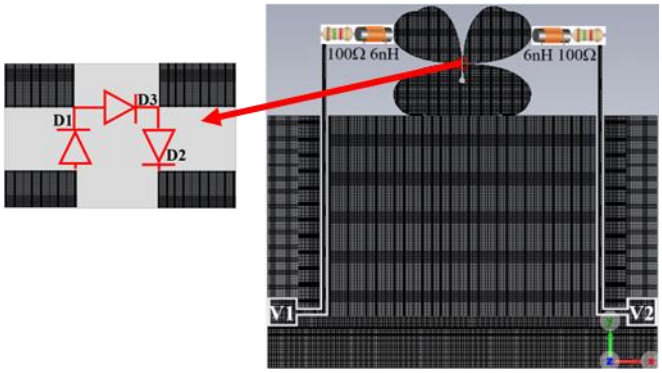

(a)

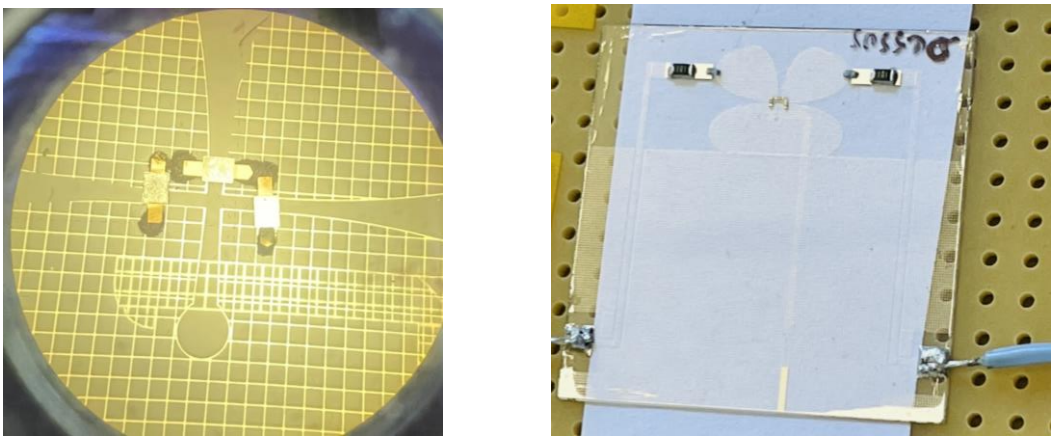

(b)

Fig. 7. Photomask **(a). (b)** General overview of the fabricated transparent antenna printed on fused quartz substrate.

Table 2. Configuration modes

Modes	Configurations modes			
	V1	V2		
Mode 1	> 0	< 0	V1 > V2	V1 =2.9 V, V2= -2.9 V
Mode 2	< 0	< 0	V1 < V2	V1 = -4.3 V, V2= -2.9 V
Mode 3	> 0	> 0	V1 < V2	V1 =2.9 V, V2= 4.3V

6. Results and discussion

The mesh antenna underwent an optical transparency test using a UV/Visible spectrophotometer. The results showed a transparency of 76% across the visible light spectrum of 400-800 nm. This confirms the high optical transparency of the mesh antenna. Fig. 6b displays the results of the test. The mesh antenna's ability to transmit visible light with minimal absorption ensures its suitability for optical applications. The high transparency is a testament to its quality and effectiveness. Fig. 8 describes the comparison between simulations and actual measurements of the performance of a transparent antenna in different operating modes (1, 2, and 3). The results of the measurements given in fig. 8 match the expected results from the simulations, showing that the antenna can operate within a frequency range of approximately 20 to 30 GHz with a low level of reflection (indicated by a magnitude of S11 lower than -10 dB) for both cases, passive and

Preprints (www.preprints.org) | NOT PEER-REVIEWED | Posted: 10 May 2023 doi:10.20944/preprints202305.0765.v1

active antennas. However, some fluctuations, or ripples, in the experimental measurements may be observed due to errors in the measurement process or losses incurred by active components in the antenna. Despite these issues, the measurements provide evidence for the wide frequency bandwidth and overall performance of the transparent antenna.

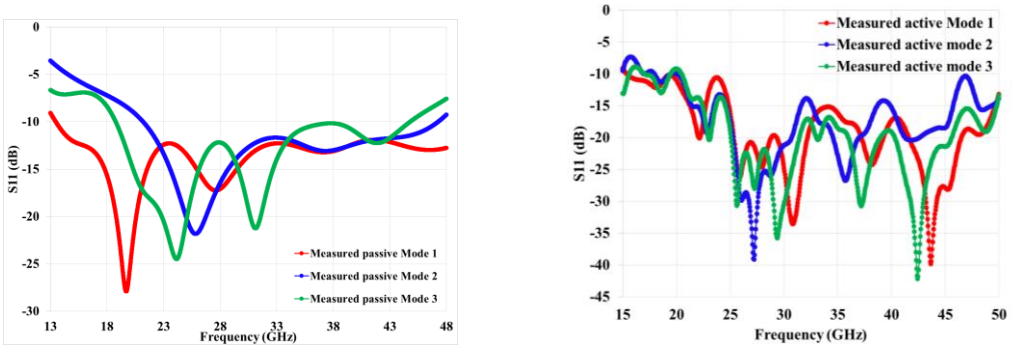

(a) **(b)**

Fig. 8. Measured return loses of the passive **(a)** and active **(b)** transparent antennas

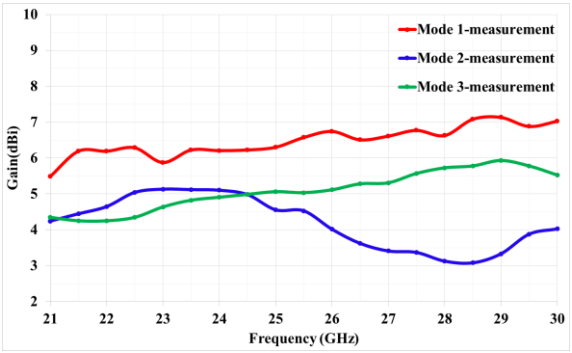

Fig. 9. Measured gain of the transparent antenna operating in Mode 1,2 et 3

The measurement results for the gain of the antenna in each mode are depicted in the figure 9. Mode 1 shows the highest gain of 7.2dBi at 26GHz, while modes 2 and 3 have a peak gain of 5.1dBi at 24 GHz and 6dBi at 29GHz respectively. The difference in gain can be explained by the higher level of rear radiation in modes 2 and 3.

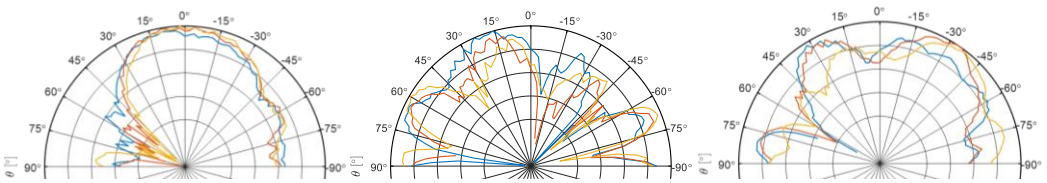

(a) (b) (c)

Fig. 10. Measured radiation patterns of active transparent antenna operating in **(a)** Mode 1, **(b)** mode 2 and **(c)** mode 3

Fig. 10 shows that by changing the DC bias of diodes, the orientation of radiation pattern change as expected.

Preprints (www.preprints.org) | NOT PEER-REVIEWED | Posted: 10 May 2023 doi:10.20944/preprints202305.0765.v1

7. Modes combination

The radiation beams of mode 1 are more directional compared to the other two modes, as the ground plane serves as a better reflector for this mode. To achieve equalization of the radiation modes in our proposed structure, we modified the values of the PIN diodes bias, which act as variable resistors, to regulate the opening of the radiation beams for mode 1. To simulate the 2D diagrams for the first mode, we varied the resistor values on the right and left at a frequency of 26 GHz.

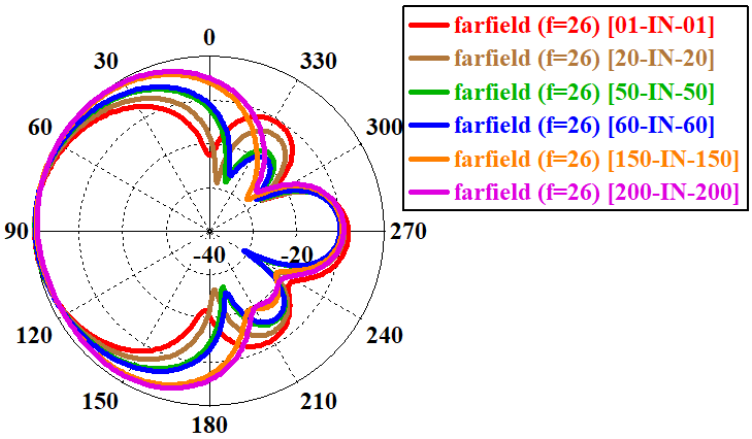

Fig. 11. Radiation patterns of mode 1 versus 3 diodes biasing. X-IN-X means, X equivalent resistor of diode and IN infinit value of equivalent diode resistor.

According to Figure 11, we have the ability to regulate the aperture of the beam. When the resistor value is X=0.01 Ω, the beam aperture is 75° at -3 dB. Conversely, when the resistor value is 200 Ω, the beam aperture increases to 155°, which is approximately twice the previous value. The table below illustrates the values of the resistors and their corresponding -3 dB beam aperture angles (θ-3dB).

Table 3. Configuration

R=R2=R3	θ-3 dB
0	75
20	84
50	99
60	104
150	145
200	155

By referring to Figure 12, we can observe the amalgamation of the three radiation modes, resulting in a coverage angle of 330°. However, the remaining coverage is obscured by the connector.

Preprints (www.preprints.org) | NOT PEER-REVIEWED | Posted: 10 May 2023 doi:10.20944/preprints202305.0765.v1

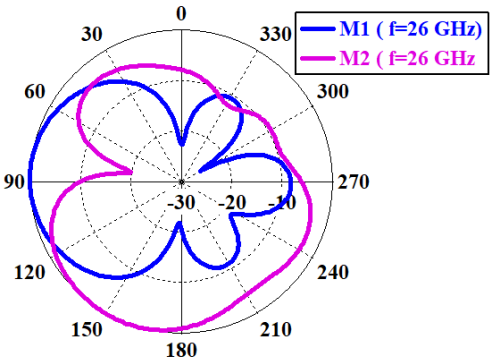

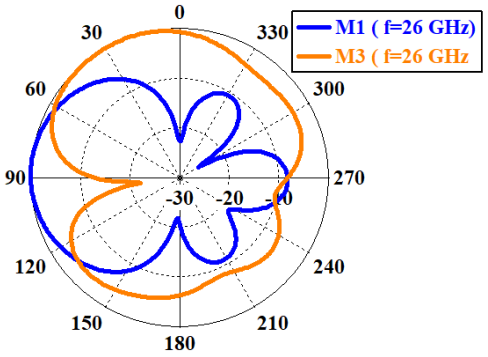

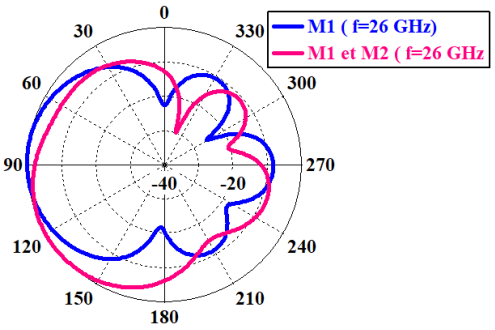

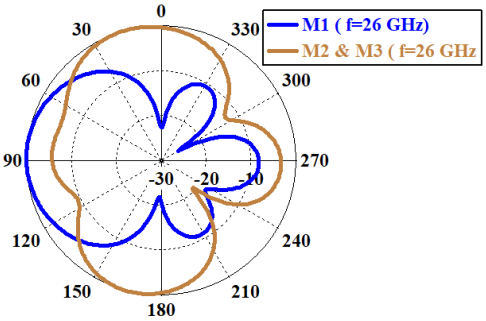

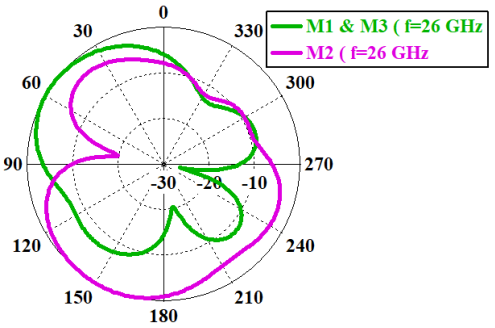

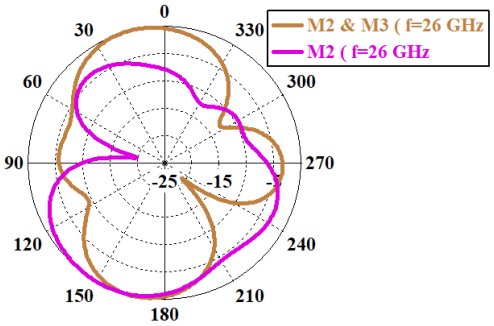

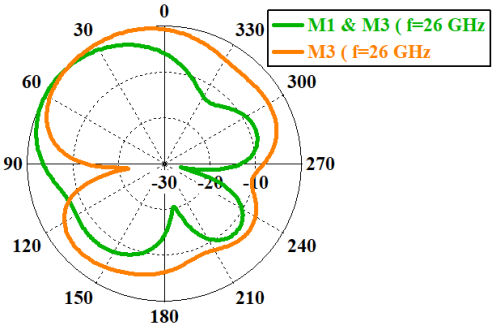

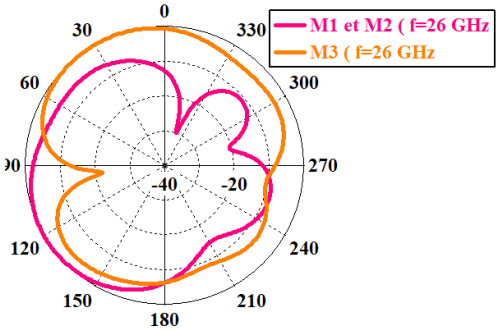

 doi:10.20944/preprints202305.0765.v1

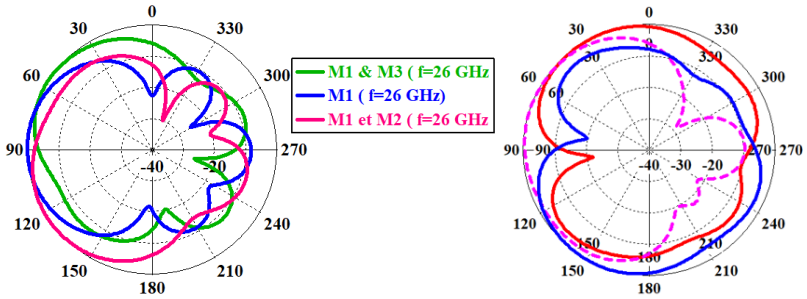

Fig. 12. Radiation patterns of different combination of modes.

8. Conclusion

The design of a compact and transparent Vivaldi antenna, suitable for use in the 20-30 GHz microwave frequency range, has been achieved. The antenna boasts a high level of transparency, with 76% visible light transmission. The beam direction of the antenna can be adjusted up to 300° by activating specific PIN diodes. Therefore, Active transparent antennas can be utilized in 5G and 6G communication systems that need multi-beam and directional beam capabilities.

Author Contributions: Conceptualization, A.C. and M.H.; methodology, A.C. and M.H.; software, A.C.; validation, A.C., M.H.; investigation, A.C. and M.H.; data curation, A.C.; writing—original draft preparation, A.C.; writing—review and editing, A.C., M.H., X.C., Q.S., S.D., F.C.; visualization, X.X.; supervision, M.H.; project administration, M.H. All authors have read and agreed to the published version of the manuscript

Funding: Not Applicable.

Data Availability Statement: Not Applicable.

Acknowledgment

This work is supported by the European Union through the European Regional Development Fund (ERDF), the Ministry of Higher Education and Research, the Région Bretagne, the Département des Côtes d'Armor and Saint-Brieuc Armor Agglomération, through the CPER Projects 2015-2020 MATECOM and SOPHIE / STIC & Ondes.

Conflicts of Interest: Declare conflicts of interest or state "The authors declare no conflict of interest." Authors must identify and declare any personal circumstances or interest that may be perceived as inappropriately influencing the representation or interpretation of reported research results. Any role of the funders in the design of the study; in the collection, analyses or interpretation of data; in the writing of the manuscript; or in the decision to publish the results must be declared in this section. If there is no role, please state "The funders had no role in the design of the study; in the collection, analyses, or interpretation of data; in the writing of the manuscript; or in the decision to publish the results".

References

[1] X. Castel, M. Himdi, and F. Colombel, "Comparison of the microwave performance of transparent monopole antennas made of different transparent conducting films," in IEEE Conf. Antenna Meas. Appl. (CAMA), Sept. 2018, Västeras, Sweden.

[2] A. Martin, O. Lafond, M. Himdi, and X. Castel, "Improvement of 60 GHz transparent patch antenna array performance through specific double-sided micrometric mesh metal technology," IEEE Access, vol.7, no.1, pp. 2256-2262, Jan. 2019.

[3] H. A. Elmobarak, S. K. A. Rahim, M. Himdi, X. Castel, and M. Abedian, "A transparent and flexible polymer-fabric tissue UWB antenna for future wireless networks," IEEE Antennas Wirel. Propag. Lett., vol.16, no.1, pp.1333-1336, May 2017.

[4] A. Martin, C. Gautier, X. Castel, and M. Himdi, "Transparent and miniature FM antenna in printed technology," Intern. J. Microw. Wirel. Technol., vol.10, no.1, pp.19-24, Feb. 2018.

[5] A. Cherif, M. Himdi, S. Dakhli, X. Castel, and F. Choubnani, "Broadband reconfigurable Vivaldi antenna for 5G communication," in Intern. Conf. IEEE WAMICON 2022, April 2022, Tampa, USA.

[6] A. Delphine, M. Rijal Hamid, N. Seman and M Himdi, "Broadband cloverleaf Vivaldi antenna with beam tilt characteristics," Int. J. RF Microw. Comput. Aided Eng., vol.30, no.5, pp.e22158, May 2020.

[7] M. R. Hamid, and P. Gardner, "Vivaldi antenna with integrated switchable band pass resonator," IEEE Trans. Antennas Propag., Vol.59, no.11, pp. 4008-4015, Nov. 2011.

[8] S. Saleh, W. Ismail, I. S. Z. Abidin, M. H. Jamaluddin, M. Bataineh, and A. Alzoubi, "Compact reconfigurable ultra wide band and 5G narrow band Vivaldi tapered slot antenna," in IEEE Intern. RF and Microw. Conf. (RFM), Dec. 2020, Kuala Lumpur, Malaysia.

[9] R. Elmahraoui, R. Rais and T. Mourabit, "A new endfire phased array based on Vivaldi antenna for 5G applications," in 19th Intern. Symp. Antenna Technol. App. Electromagn. (ANTEM), Aug. 2021, Winnipeg, MB, Canada.

[10] J. Guo, S. Xiao, S. Liao, B. Wang, and Q. Xue, "Dual-band and low profile differentially fed slot antenna for wide-angle scanning phased array," IEEE Antennas Wirel. Propag. Lett., vol.17, no.2, pp.259-262, Dec 2017.